Synthesis of N-CNT/TiO_2 composites thin films: surface analysis and optoelectronic properties

Hamza Belkhanchi[1], *Younes* Ziat[1*], *Maryama* Hammi[2**], *Charaf* Laghlimi[3], A*bdelaziz* Moutcine[3], *Anas* Benyounes[4], and *Fouzia* Kzaiber[1]

[1]Laboratory of Engineering and Applied Technologies, Higher School of Technology, Sultan Moulay Slimane University, Beni Mellal, Morocco
[2]Laboratory of Materials, Nanotechnologies and Environment, Department of Chemistry, Faculty of Sciences, University of Mohammed V, Rabat, Morocco
[3] Molecular Electrochemistry and Inorganic Materials Team, Beni Mellal, Faculty of Science and Technology, Sultan Moulay Slimane University, Morocco
[4]Department of Chemistry, Faculty of Sciences, University of Mohammed V, Rabat, Morocco

Abstract. In this study, we have investigated the surface analysis and optoelectronic properties on the synthesis of N-CNT/TiO_2 composites thin films, using sol gel method for a dye synthetized solar cell (DSSC) which is found to be simple and economical route. The titanium dioxide based solar cells are an exciting photovoltaic candidate; they are promising for the realization of large area devices. That can be synthetized by room temperature solution processing, with high photoactive performance. In the present work, we stated comparable efficiencies by directing our investigation on obtaining Sol Gel thin films based on N-CNT/TiO_2, by dispersing nitrogen (N) doped carbon nanotubes (N-CNTs) powders in titanium tetraisopropoxyde (TTIP). The samples were assessed in terms of optical properties, using UV—visible absorption spectroscopic techniques. After careful analysis of the results, we have concluded that the mentioned route is good and more efficient in terms of optoelectronic properties. The gap of "the neat" 0.00w% N-CNT/TiO_2 is of 3eV, which is in a good agreement with similar gap of semiconductors. The incorporated "w%N-CNTs" led to diminishing the *Eg* with increasing N-CNTs amount. These consequences are very encouraging for optoelectronic field.

1 Introduction

Carbon nanotubes are the subject of many investigations in various areas such as composite materials [1-3], in the (Li ion) batteries to increase their performance [4], the storage of the energy [5], optic [6] and photovoltaic [7]. And for the photovoltaic field, there are several important characteristics that need to be considered for a photocatalyst as TiO_2 in dye sensitized solar cells (DSSC), it is crucial to be able to transfer holes from the sensitizing dye after the dye has injected electrons in the titanium dioxide (TiO_2). On the other hand, DSSCs

Corresponding author:*ziat.estbm@gmail.com; **mar.hammi@yahoo.com

based on nanostructure materials offer very low cost and relatively efficient photovoltaics' energy conversion [8]. The used routes don't embody any inconvenient to the dye layer on the titanium dioxide nano crystallites [9]. Due to its ecofriendly production, the DSSCs are extensively studied for the reliable and safe energy source [10].

In this study, we have shown that the TiO_2 and N-CNT composed an active layer, and the electrons recombination procedure may affect the best conversion of DSSCs' efficiency. Given that the nitrogen doped CNT has a special structure and can conduct electrons at room temperature (RT). Where the electrons are generated from TiO_2 under light irradiation, the N-CNT compound can also easily conduct photoelectrons. The analysis of the present results concluded that the sol gel route is good and more efficient in terms of optoelectronic properties.

This work provides new insights into the development extrinsic semiconductors, which attracts great interest in the current solar nanotechnology. Indeed, nitrogen doped carbon nanotubes (N-CNTs) are known by their large surface area, high electrical conductivity and chemical stability. These properties have provided to N-CNTs potential applications in N-CNT-based composites which are used as candidates for nanoelectronic devices. In fact, the synergistic effect of N-CNTs and TiO_2 is caused by the improved photocatalytic activity through reducing recombination efficiency of electron-hole pairs.

2 Synthesis

The "hybrid CNTs" were synthesized within catalytic chemical vapor deposition in a fluidized room reactor by ethylene C_2H_4 as carbon source and acetonitrile/N_2 as nitrogen/carbon source. The experiment carried out initially with C_2H_4 (650 ml/min) for ½ hour aimed at producing CNT. And the N-CNTs were produced from acetonitrile/N_2 for 35 min. The carbon nanotubes were purified via aqueous solution of Sulfuric acid 'H_2SO_4' – 50 vol % under refluxes for 3h 10min.

For titanium isopropoxyde ($C_{12}H_{28}O_4Ti$), the coated solution is obtained by dissolving 3ml of $C_{12}H_{28}O_4Ti$ from Aldrich 98% 6ml of isopropanol: C_3H_8O, then different 'weight' percent (%) of N-CNTs powders (0.09; 0.25 and 0.4wt %) were dispersed in the obtained solution. This mixture is stirred at 65°C for 12min. Then, 6ml of acetic acid: CH_3COOH was added. After that, other mixture was stirred in 20min. Within 2hours, the final mixture is being stirred after adding 12ml of methanol: CH_3OH to have the Sol Gel solution. This latter was spincoated on indiumtinoxide (ITO) glass substrates. The ITO should be etched with detergent, followed by ultrasonic cleaning for few minutes, then rinsed with deionized water and finally steaming at 110 °C for 10 minutes. Then, the annealing temperature has been elevated from 100 – 500°C.

3 Specific area and pores diameter within BET and BJH schemes

The mesoporous structure of TiO_2 was examined within the pores diameter calculations and surface area. The multipoint N_2gas sorption is experimented at 77K to examine the specific area and pores diameter of the synthesized TiO_2 via the "micromeritics ASAP2010". The specific surface calculations are based on Brunauer, Emmett et Teller (BET), which is expressed by [11]:

$$S_{BET} = n_m^a \times N \times a_m \quad (1)$$

The n_m^a is the monolayer capacity, where a_m presents the molecular crosssectional area. N stands for *Avogadro constant*. The pore size distribution was obtained by t the Barrett, Joyner, and Halenda (BJH) scheme [12]. For BJH, the sorption data in the relative pressure

range from 0.05-0.25, the calculating pore size distributions is from empirical isotherms via the Kelvin model of pore filling. It is applicable only to the small macro pore size and mesopore range. Hence, the Table 1 shows the evolution of "surface area" and "pores diameter" versus annealing temperatures.

Table 1. Pore diameter and specific surface area of TiO_2 associated to annealing temperature.

Annealing temperature (°C)	Pore diameter PD(nm)	Specific area (SBET$m^2.g^{-1}$)
100	1.95	205
300	2.09	160
500	4.86	125

As noticeable through Table 1, The increase of annealing temperature augments give rise to pores diameter (P_D) which reaches the maximum up to 500 °C. Thermal treatment of the powders at 500°C leads to a systematic decrease of the SBET values and a considerable enlarging of the average pore size. So, to keep high SBET, the annealing temperature is limited to 300 °C at which crystal growth was slightly affected, these data suggest the difference in porosity can affects their sorption and photocatalytic behaviors of TiO_2.

4 Optical characterization and Swanepol method

The absorption spectroscopic technique, enable us to record the optical transmission of the layers as a function of wavelength, and determining the value of the optical gap (*Eg*) of the layer as well as the refractive indices of the films. For this purpose, the following formulas are given by the method of Swanepol and Manifacier [13-14].

$$d = \left(\frac{\lambda_1 \lambda_2}{2(\lambda_1 n_2 - \lambda_2 n_1)}\right) \quad (2)$$

where d is the thickness of the film. n_1 and n_2 present, respectively, the refractive indices of the films for λ_1 and λ_2 "adjacent wavelengths". Titanium oxide is a transparent material, whose refractive index in bulk form is equal to 2.5 (anatase phase) [15]. Whereas, in the form of a thin layer, its refractive index varies according to the conditions of preparation. According to the authors [16-17], the refractive index varies between 1.9 and 2.5.

In this work, we assume that the deposited thin films are homogeneous. The porosity of thin films is calculated from the following equation [18].

$$Porosity = \left(1 - \frac{n^2 - 1}{n_D^2 - 1}\right).100(\%) \quad (3)$$

Where n_D is the refractive index of pore-free TiO_2[19], and n is the refractive index of porous thin films. From this equation, we can assume the relationship between the refractive index and the porosity. Low porosity lead to the increase of *n*. Thus, in order to have remarkably higher refractive indexes, our films must be highly densified.

The refractive indices in the spectral region of transparency is expressed by:

$$n_1 = \left[N_1 + (N_1^2 - S^2)^{1/2}\right]^{1/2} \quad n_2 = \left[N_2 + (N_2^2 - S^2)^{1/2}\right]^{1/2} \quad (4)$$

Where N is the *Swanepoel* coefficient in the transparent spectral region. And S is the refractive index of the glass.

$$N_1 = 2S\left(\frac{T_{max1} - T_{min}}{T_{max1} \times T_{min}}\right) + \left(\frac{S^2+1}{2}\right) \quad N_2 = 2S\left(\frac{T_{max2} - T_{min}}{T_{max1} \times T_{min}}\right) + \left(\frac{S^2+1}{2}\right) \quad (5)$$

Where T_{max} and T_{min} are the maxima and minima of the transmittance curve. To predict the absorption (α) in terms of transmittance (T), we have the following formula

$$\alpha = \frac{1}{d} ln \left(\frac{100}{T}\right) \qquad (6)$$

4.1 Transmittance and the optical gap E_g

For the fields of spectroscopy, we can distinguish the ultraviolet (UV), infrared (IR) and microwave. In the present study, we used a double beam recording spectrophotometer for UV—Visible spectral "300—800nm". The transmittance (T) presents the ratio of transmitted light intensity to the incident light intensity. To plot the spectra, a blank substrate was used in the reference beam of the spectrophotometer, a computer device is connected to this unit enable us to visualize imitates the spectra which are representing the transmittance (T) of the film.

The obtained spectra of transmittance (T) connected to N-CNTs/TiO_2 composites were plotted (Fig. 1). This figure shows typical spectra of N-CNTs/TiO_2 in the range of 300—800nm with different "N-CNTs wt %". At this point, it is concluded that the T decreases with increasing the incorporated N-CNTs in wt%. The obtained film shows a high transmittance for TiO_2thin film, it is of 77.5%. And $T$is of 61% for the "0.40 wt% N-CNT/TiO_2"composite.

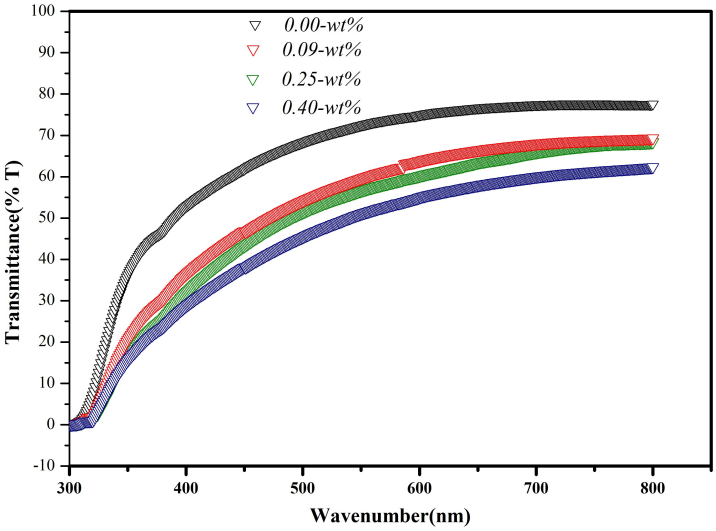

Fig. 1. The transmittance (T) versus wavenumber for 0.00; 0.09; 0.25 and 0.40 wt% N-CNTs/TiO_2 composite

In the UV range, the abrupt decrease in film transmittance is due to the fundamental absorption of light. It corresponds to transitions between valence band towards the conduction band when there is excitation charge carriers. Beyond the fundamental absorption threshold, the absorption coefficient follows a variation with the energy ΔEg, which is expressed by the following relation [20]:

$$\Delta E_g = \frac{h^2}{8m^*}\left(3n/\pi\right)^{2/3} \qquad (7)$$

Where h stands for the Planck constant, m^* refers to the effective mass of the carriers and $n$is the concentration of free electrons.

From the transmittance spectra, we can calculate the optical gap (*Eg*) value of semiconductors from Tauc method [21]. Where the wavelength composing white light are scanned via the spectrophotometer and electromagnetic radiation interacts with matter. The IR causes vibrational transitions in molecules while the UV—Vis cause electronic transitions. Then the absorptions start to consider the band gap of the semiconductors. Graphically, it is possible to define the optical gap within the followed formula [22-24].

$$(\alpha h\nu) = B(h\nu - Eg)^n \quad (8)$$

h, *ν, α, n* and B present the "Planck constant, vibration frequency, absorption, the power factor and B is a proportional constant", respectively. The curves of $(\alpha h\nu)^2$ as function of energy $(h\nu)$ characterize a linear portion whose intersection with the axis of h*ν*, gives the optical gap. From the *T* spectra, we have the *Eg* of the N-CNTs/TiO_2 composites, see (Fig. 2).

N-CNTs fillers contents were indicated on (Fig. 2. a, b, c and d). The gap of "the neat" 0.00w% N-CNT/TiO_2 is of 3eV, which is in a good agreement with similar gap of semiconductors [25]. Due to the augmentation of the fillers content, the optical gap values are reduced from (Fig. 2.a to Fig. 2.d). Clearly in the same figure, we showed the determination of optical gap by the extrapolation from variation of $(\alpha h\nu)^2$ versus h*ν*. Hence, the incorporated "N-CNTs wt%" led to diminishing the *Eg* with increasing N-CNTs amount.

Similar behavior of band gap energy is expressed by TiO_2/MWCNT nanocomposites [26]. However, our studied composites revealed larger absorption and shift towards shorter wavelengths.

These consequences are very encouraging, therefore we have focused our attention on the front of a solar cell component, by performing the electrical measurements of the obtained thin films.

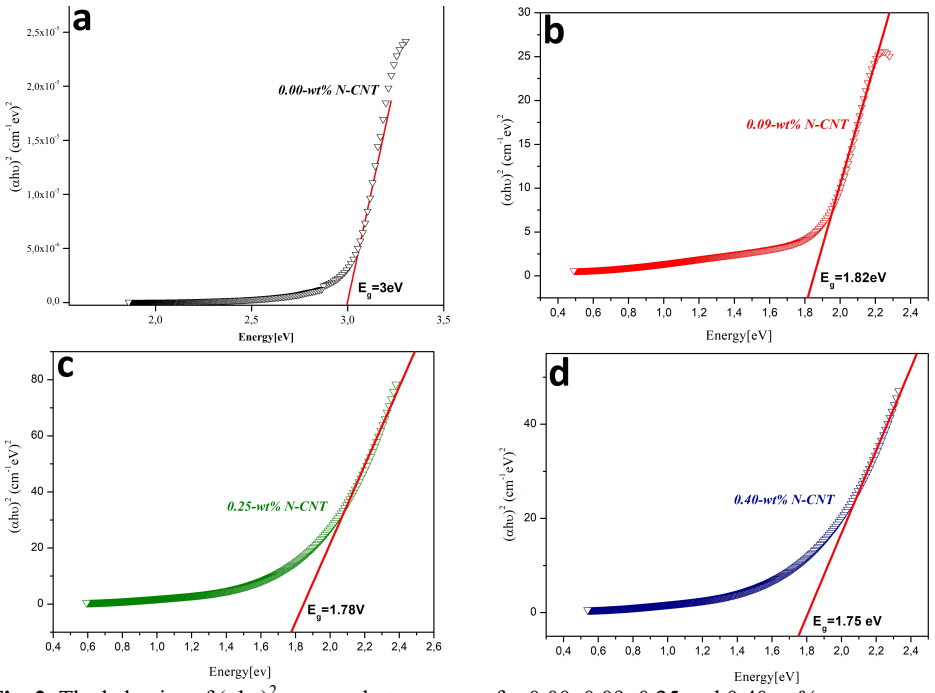

Fig. 2. The behavior of $(\alpha h\nu)^2$ versus photon energy for 0.00; 0.09; 0.25 and 0.40 wt%

4.2 Sheet conductivity behaviour in "wt% N-CNTs/TiO_2" composite gap

The obtained N-CNTs/TiO_2 composite were investigated in the surface conductivity point of view, which is extracted from surface resistivity recognized as sheet resistance defined by the followed formula [17]:

$$R_{\square} = \rho \times d^{-1} \quad (9)$$

Where ρ is the resistivity. The film prepared by solgel route using different amount of % N-CNT exhibited an early threshold conduction at 9%, which gives a good promising thin film in the terms of the conductivity electric, see (Fig. 3).

It is noted that the reduction of resistivity involves an augmentation in the carrier concentration. Increasing the quantity of carriers leads to an augmentation in the visible absorption, then increasing the figure of merit (FOM) of the present thin films based on N-CNTs/TiO_2. The transparent conductive oxides (TCO) are extensively used in solar cell fields, to get high quality TCO films, it is important to define the (FOM) for qualifying those layers of films and predicting the influence of the used TCO films on solar cells process. The obtained results are validated with the optical properties of the elaborated "N-CNTs/TiO_2" composite. These findings supposed that those thin films are good candidates for the optoelectronics field.

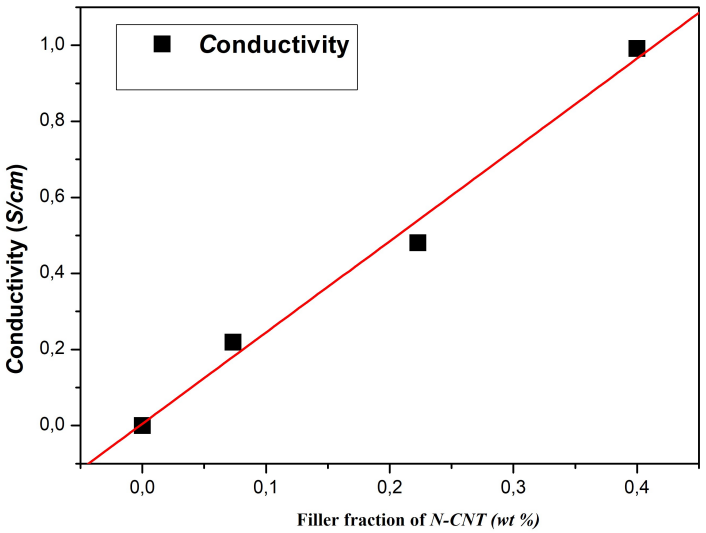

Fig. 3. Variation of average conductivity in wt% "N-CNTs/TiO_2"

According to (Fig. 3), it is noteworthy that electrical conductivity of unloaded thin film is of the order of 10-9S/cm. It is linearly enhanced when the concentration of incorporated N-CNTs are elevated. Typical behavior is expressed by TiO2 based thin films as shown by [27], they observed decrease in sheet resistance with increasing number of deposited bilayers indicates that the MWCNT/TiO2 films become more conductive. They attribute this increase in conductivity to an increase in MWCNTs in the films and, more importantly, to the increased percolation of MWCNTs within the nanocomposite film as more bilayers are deposited. This evolution is more probably due to number carriers increase within TiO2 host matrix. Therefore, the gap must drop significantly, in good agreement with Burstein - Moss theory [28, 29].

5 Conclusion

For the N-CNT/TiO_2 composites, the synthesis, specific area and pores diameter within BET and BJH schemes were described. The current study was based on the solgel elaboration, since it is efficient route. The optical characterization and Swanepol method were discussed. The obtained spectra of *T* connected to N-CNTs/TiO_2 composites shows typical spectra in the range of 300—800nm with different "N-CNTs wt %". The obtained film shows a high transmittance for TiO_2 thin film, it is of 77.5%. And T of 61% for the "0.40 wt% N-CNT/TiO_2"composite. The gap of "the neat" 0.00w% N-CNT/TiO_2 is of 3eV, which is in a good agreement with similar gap of semiconductors. The incorporated "w%N-CNTs" led to diminishing the *Eg* with increasing N-CNTs amount. It is noted that the reduction of resistivity involves an augmentation in the carrier concentration. Increasing the quantity of carriers leads to an augmentation in the visible absorption. These consequences are very encouraging for optoelectronic application.

Acknowledgements: The authors would like to thank Ms. ***Maryem*** **Errachid** from "Economy Management, Mohammed V University of Rabat, Faculty of Law, Economics and Social Sciences-Souissi, Rabat, Morocco" and Ms. ***Saloua*** **Rzaoudi**, from "Economic sciences and of management, Polydisciplinary Faculty, Sultan Moulay Sliman University, Beni Mellal, Morocco"to accept the language revision.
Our thanks are extended to "the mechatronic department, Higher School of Technology, Sultan Moulay Slimane University, Beni Mellal, Morocco", especially, the professors ***Fatima Zahra*** **Baghli** and ***Yassine*** **Lakhal** for the fruitful discussion.

References

1. D. Xu, G. Luo, J. Yu, W. Chen, C. Zhang, D. Ouyang, Y. Fang, X. Yu, J. Alloys Compd**702**, 499(2017)
2. S. Aror, N. Kumari, C. Srivastava, J. Alloys Compd**801**, 449(2019)
3. T. Zhao, X. Peng, X. Zhao, J. Hu,T. Jiang, X. Lu, H. Zhang, T. Li, I. Ahmadc, J. Alloys Compd**817**, 153057 (2020)
4. Y. Ziat, A. Benyounes, O. El Rhazouani, C. Laghlimi, M. Hammi, Turk. J. Mater **3**, 61 (2018)
5. C. T. Hsieh, H. Teng, W. Y. Chen, Y. S. Cheng, Carbon **48**, 4219(2010)
6. A. Shabaneh, S. Girei, P. Arasu, M. Mahdi, S. Rashid, S. Paiman, M, Yaacob, Sensors **15**, 10452 (2015)
7. H .Derbal-Habak , C. Bergeret, J. Cousseau, J. M. Nunzi, Sol. Energy Mater. Sol. Cells **95**,S53(2011)
8. B. Kiliç, E. Gür, S. Tüzemen, J. Nanomater**7**, ID 474656(2012)
9. M. N. Amalina, N. A. Rasheid, and M. Rusop, J. Nanomater**6**, ID 637637 (2012)
10. M.S. Ahmad, A. K. Pandey, N.A. Rahim, Renew. Sust. Energ. Rev **77**,89(2017)
11. J. Rouquerol, D. Avnir, C. W. Fairbridge, D. H. Everett, et al, Pure. Appl. Chem **66**, 1739 (1994)
12. R. Bardestani, G. S. Patience, S. Kaliaguine, Can. J. Chem. Eng**97**, 2781(2019)
13. R. Swanepoel, J. Phys. E: Sci. Instrum**16**, 1214(1983)
14. J. C. Manifacier, D. M. Murcia, J.P. Fillard, E. Vicario, Thin solid films **41**, 127(1977)
15. M. D. Hernandez-Alonso M. D. Hernandez-Alonso Isabel T. Tejedor, J. M. Coronado, J. Soria, M. A. Anderson, Thin Solid Films **502**, 125 (2006)
16. A. Turković, M. Ivanda, J. Tudorić-Ghemo, N.Godinović, I. Sorić, In Proceedings of Symposium A 3 of the International Conference on Advanced Materials (ICAM 91) Non-Stoichiometry in Semiconductors(1992)
17. S. Balaji, Y. Djaoued, J. Robichaud, J. Raman Spectrosc**37**, 1416 (2006)

18. T. Ohsaka, S. Yanaoka, O. Shimomura, Solid State Commun**30**, 345 (1979)
19. M. H. Liao, J. Solid. State. Chem **179**, 2020 (2006)
20. J. Mass, P. Bhattacharya, R.S. Katiyar, Mat. Sci. Eng. B-Adv **103**, 9 (2003)
21. J. Tauc, A. Menth, J. Non-Cryst. Solids **8**, 569 (1972)
22. Y. Ziat, A. Abbassi, M. Hammi, A. Ait Raiss, O. El Rhazouani, Opt. Quantum Electron**48**, 511 (2016)
23. A. Benyounes, M. Hammi, Y. Ziat, A. Slassi, N. Zahra, Appl. Phys. A **90**, 124 (2018)
24. Z. Zarhri, M. ÁngelAvilésCardos, Y. Ziat, M. Hammi, O. El Rhazouani, J. Cesar Cruz Argüello, D. Avellaneda Avellaneda, J. Alloys Compd**819**, 153010 (2019)
25. M. Hammi , A. Abbassi, Mater. Lett**166**, 206(2016)
26. M. B. Askari, Z.T. Banizi, M. Seifi, S. B. Dehaghi, P. Veisi, Optik**149**, 447 (2017)
27. K. E. Tettey, M. Q. Yee, D. Lee, ACS Appl. Mater. Interfaces **2**, 2646 (2010)
28. B. Šantić, A. Moguš-Milanković, D.E. Day, J. Non-Cryst. Solids**296**, 65 (2001)
29. D. M.Tawati, M. J. B. Adlan, M. J. Abdullah , J.Non-Cryst. Solids **357**, 2152 (2011)